Modeling of an Optocoupler-Based Audio Dynamic Range Control Circuit

Felix Eichas and Udo Zölzer

Department of Signal Processing and Communications, Helmut Schmidt University, Holstenhofweg 85, Hamburg, Germany

ABSTRACT

Virtual analog modeling is the process of creating a digital model of an analog system. In this work a virtual analog model of a dynamic range compression circuit for electrical guitars is constructed by analyzing and measuring the analog reference system. The particular property of the chosen compression system is the use of an analog optical isolator, also called optocoupler. It is a two-port circuit element used to electrically isolate different parts of the audio system while maintaining one-directional coupling via the optical channel. The used analog optical isolator was a Perkin Elmer VTL5C2, consisting of a light dependent resistor and a light emitting diode in an opaque enclosure.

All the characteristics of the nonlinear elements were measured, especially the VTL5C2, then the circuit was analyzed to determine its static behavior. In the digital model the output signal is multiplied with a time-variant gain factor, which is dependent on the input signal. Several processing blocks are used to calculate the gain factor, emulating the static and dynamic behavior of the analog reference system. An iterative error minimization procedure is used to refine parameters for the digital model. Finally the output of digital model and analog reference are compared to show how well the model has been adapted to the reference device.

Keywords: Virtual Analog Modeling, Circuit Analysis, Circuit Modeling, Analog Optical Isolators, Dynamic Range Compression

1. INTRODUCTION

Photo-resistive optical isolators are systems consisting of a light-source (typically a light emitting diode (LED)) and a photo-resistor making them optically coupled while they are electrically isolated. They have been used in analog audio systems since the early 1960s when J.F. Lawrence combined a photo-resistor and a light source to form an analog optical isolator (AOI). The Teletronix LA-2A was the first (tube-based) optical limiting amplifier using an analog optical isolator. The AOI built for the LA-2A is called T4 cell. The principle of this compressor is the same as for most optical compression systems. The amplification of the input signal is driven by the modified output signal.[1]

Since the compression system is tube-based and vacuum tubes are not as convenient as transistors in terms of e.g. space requirements or power supply needs, optical compression systems with transistor-based amplification became more and more popular in the *do it yourself* (DIY) guitar effect scene. From this scene originated the schematic for a very simple but rather popular gain control system for electric guitars. Introduced by John Hollis in 2001, it is a simplistic circuit with an AOI and two operational amplifiers.[2] This guitar effect device is the focus of this work.

A guitar effect, also called stompbox, is an electrical system which modifies the signal from an electric guitar or bass. It is connected between an amplifier and the instrument itself, as shown by Fig. 1. The name stompbox originates from the fact that the musician has to 'stomp' on the switch with their foot to turn the device on or off so the hands remain free to play the instrument.

In previous work about virtual analog guitar effects modeling Kröning et. al successfully modeled a commercial gain control unit for guitars, the MXR - Dynacomp.[3] The circuit was analyzed and modeled with a

Further author information:
Felix Eichas: E-mail: felix.eichas@hsu-hh.de, Telephone: +49 40 6541 2743

Novel Optical Systems Design and Optimization XIX, edited by Arthur J. Davis, Cornelius F. Hahlweg, Joseph R. Mulley, Proc. of SPIE Vol. 9948, 99480W · © 2016 SPIE
CCC code: 0277-786X/16/$18 · doi: 10.1117/12.2235686

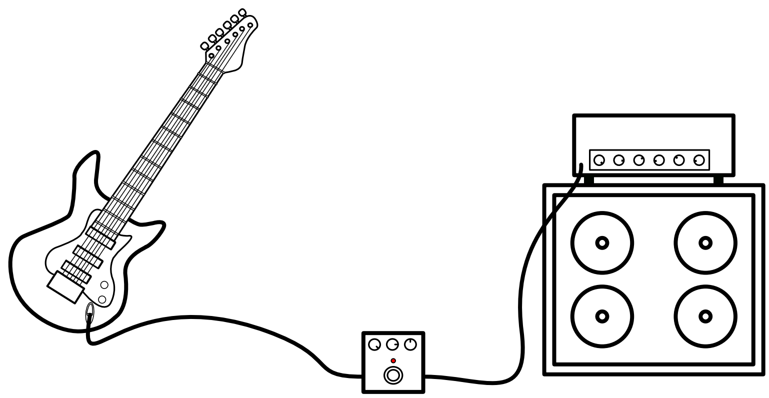

Figure 1: Typical usage of a guitar effect device.

nonlinear state-space system, which describes currents and voltages in the circuit. This technique delivers convincing results but is not very efficient in terms of computational needs, because for every time sample, a set of nonlinear equations has to be solved by an iterative nonlinear solver. To achieve a practical real-time model, circuit specific simplifications had to be made.

In this work, a generic dynamic range compressor model is adjusted with a static characteristic from the analog reference device as well as extracted attack and release time parameters. The model is extended with a linear time-invariant filter to match the frequency characteristic of the original device. All the measurements are input/output measurements, which facilitates the modeling process, especially for commercial products where a circuit diagram is not available.

In section 2 the circuit elements of the dynamic range compressor are measured and the circuit is analyzed for steady state as well as dynamic behavior. In section 3 the digital model which was used to emulate the circuit is shown. Sections 4 and 5 describe the system identification techniques, which were used to extract the system's characteristics, section 6 shows the results of the modeling process and section 7 concludes this work.

2. HARDWARE

This section covers the circuit of the flatline compressor and its analysis. First, the circuit and its nonlinear elements are shown, the measurements of the nonlinear elements are explained and afterwards the circuit is analyzed.

2.1 Non-Linear Circuit Elements

The main nonlinear element in this circuit is the analog optical isolator. An AOI consists of a light source (emitter) and a photo-sensor, in our case a photo-resistor or light dependent resistor (LDR), combined in a sealed optical channel (see Fig. 2). If no current is flowing through the light source and there is no light emitted inside the enclosure, the resistance of the photo-resistor is high ($R_{\mathrm{off}} > 1$ MΩ).[4] When the light source starts to emit light, the resistance of the photo-resistor decreases. With increasing light intensity the doped silicon surface of the photo-resistor becomes more conductive. For an LED current of $I_{\mathrm{LED}} > 40$ mA the resistance drops below $R_{\mathrm{on}} < 300$ Ω.[4] Source and sensor are only coupled via the optical channel which prohibits electrical coupling. Other nonlinear elements of the compressor are rectifier diodes in the feedback path of the second operational amplifier.

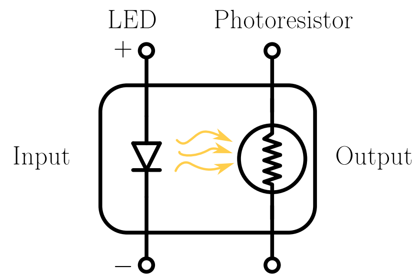

Figure 2: Schematic diagram of an analog optical isolator (AOI).

2.2 Circuit Diagram

The circuit of the compressor can be seen in Fig. 3. It can be divided into two main stages. The first, and most important stage, is the non-inverting amplifier consisting of Q_1, R_2, R_3, the **sustain** potentiometer and the resistive side of the analog optical isolator R_{LDR}. The second stage creates the control signal, which modifies the gain of the non-inverting amplifier of the first stage via the optical link of the analog optical isolator. The output of the non-inverting amplifier is used as the input signal for the second stage. Diodes D_1 - D_4 are *D9b*

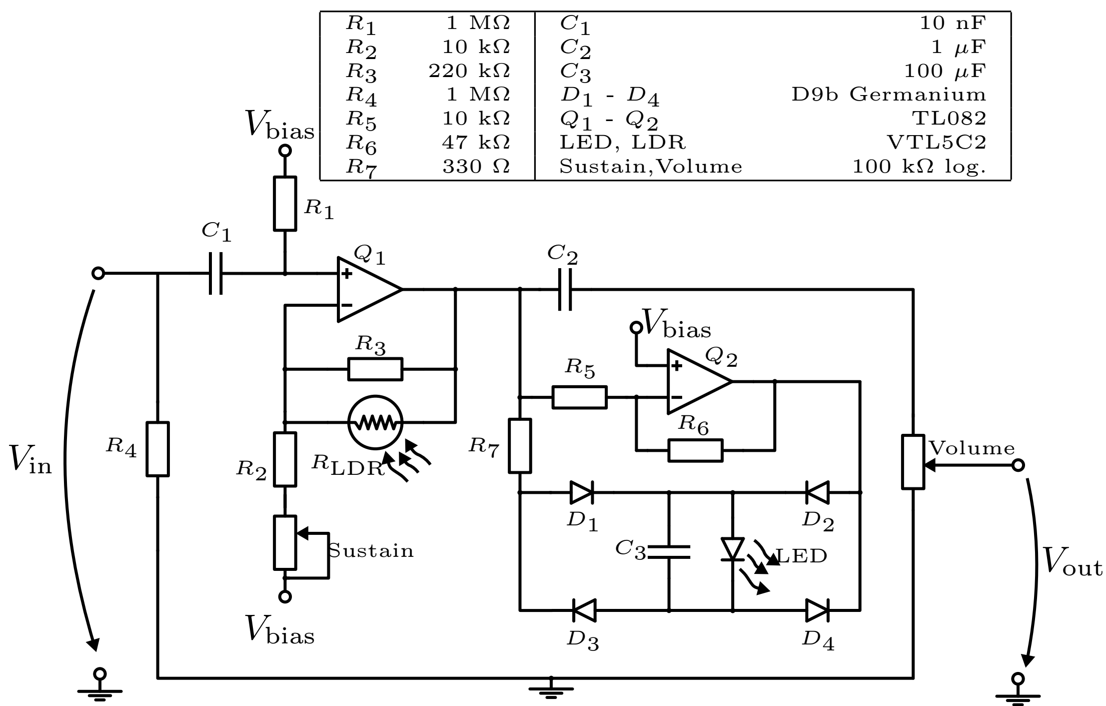

R_1	1 MΩ	C_1	10 nF
R_2	10 kΩ	C_2	1 μF
R_3	220 kΩ	C_3	100 μF
R_4	1 MΩ	D_1 - D_4	D9b Germanium
R_5	10 kΩ	Q_1 - Q_2	TL082
R_6	47 kΩ	LED, LDR	VTL5C2
R_7	330 Ω	Sustain,Volume	100 kΩ log.

Figure 3: Circuit diagram of the *flatline compressor*.

germanium diodes and the used operational amplifier is the TL082 from Texas Instruments. The bias voltage V_{bias} is set to half the supply voltage $V_{\mathrm{cc}} = 9\,\mathrm{V}$ and is used to bias the inputs of the OPs to avoid the need for a negative voltage supply.

The analog optical isolator used in this work is a Perkin Elmer VTL5C2. For readability the enclosure of the AOI is not depicted in the schematic. The light emitting input is shown as LED and the resistive element is depicted as R_{LDR}. The arrows in the circuit diagram indicate the optical path between LED and LDR.

When the output signal of the first stage rises above a certain level, the LED emits light and the resistance of the LDR decreases. This leads to a reduction of the gain of the non-inverting operational amplifier stage for higher input signal levels and thus a reduction of the dynamic range of the signal.

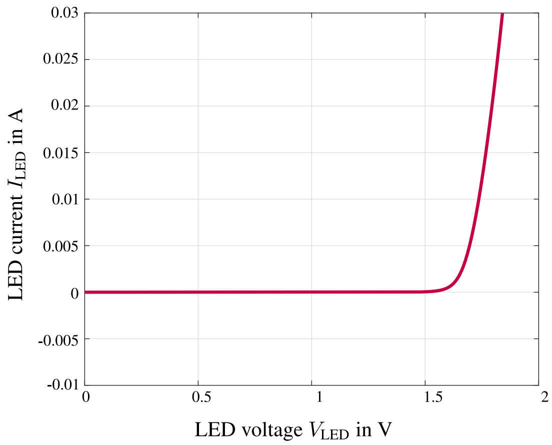

(a)

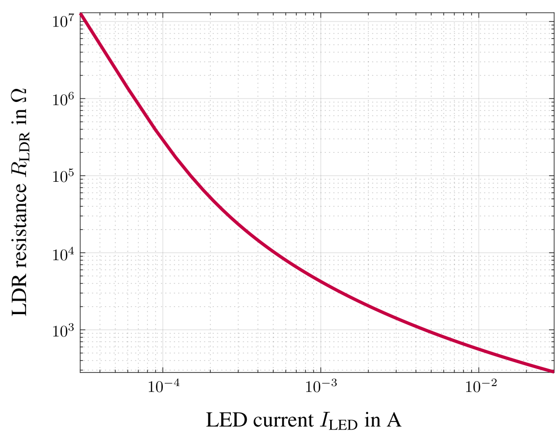

(b)

Figure 4: Measurements of the VTL5C2 (a) current-voltage characteristic of the LED (b) resistance-current plot of the LED current to LDR resistance.

2.3 Hardware Measurements

The nonlinear circuit elements were measured before assembling the circuit. The current-voltage characteristics of the *D9b* rectifier diodes were measured. All four curves matched very closely. The characteristic curves of the AOI are more important for the behavior of the circuit. The current-voltage characteristic of the light emitting diode and the value of the light dependent resistor in respect to the LED current were measured. In Fig. 4a the current-voltage characteristic of the LED is shown. When the voltage across the LED exceeds 1.6 V a current flows through it and the LED emits light.

Figure 4b shows the value of the light dependent resistor (LDR) in relation to the current flowing through the LED. If the LED is dark (low forward current), the value of the LDR is very high $R_{\mathrm{LDR}} > 1\,\mathrm{M\Omega}$ for LED currents of $I_{\mathrm{LED}} < 0.07\,\mathrm{mA}$. With increasing forward current of the LED, the light intensity increases proportionally which leads to a lower resistance of the LDR. The LDR reaches a value of $R_{\mathrm{LDR}} < 300\,\Omega$ for LED currents of $I_{\mathrm{LED}} > 30\,\mathrm{mA}$, which corresponds well with the datasheet.[4]

2.4 Circuit Analysis

The circuit is analyzed in two steps. First the static characteristic of the circuit is derived in theory, then the dynamic behavior is analyzed by measuring how the system reacts in the dynamic case of sudden changes in the input signal.

2.4.1 Static Behavior

To analyze the behavior of the circuit in the steady state, we divided the overall system into two parts. The first part is the non-inverting amplifier (around Q_1, see Fig.3). According to Kories et al.,[5] the gain for an ideal non-inverting amplifier, as shown in Fig. 5, is

$$g = 1 + \frac{R_{\mathrm{A}}}{R_{\mathrm{B}}} \quad . \tag{1}$$

The resistance R_{A} is the parallel connection of resistances R_3 and R_{LDR} which yields

$$R_{\mathrm{A}} = \frac{R_3 + R_{\mathrm{LDR}}}{R_3 \cdot R_{\mathrm{LDR}}} \quad . \tag{2}$$

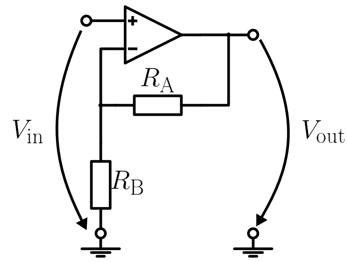

Figure 5: Non-inverting amplifier.

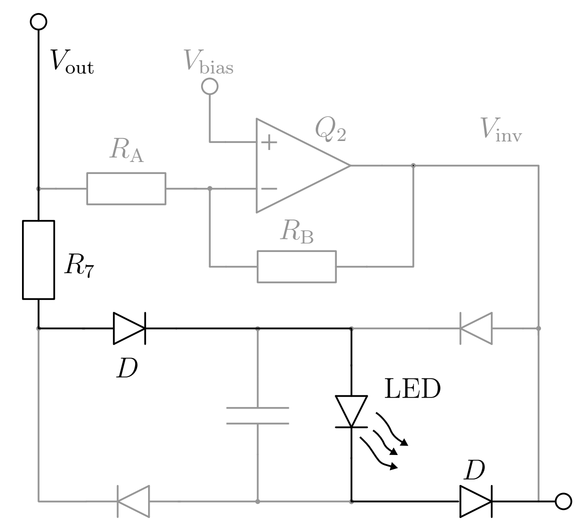

Figure 6: Second operational amplifier stage of the circuit.

The resistance R_B is the series connection of the sustain potentiometer and R_2,

$$R_B = R_2 + R_{sustain} \quad . \tag{3}$$

Inserting Eq. 2 and Eq. 3 in Eq. 1 yields

$$g = 1 + \frac{R_3 \cdot R_{LDR}}{(R_2 + R_{sustain}) \cdot (R_3 + R_{LDR})} \quad , \tag{4}$$

which is the gain of the non-inverting amplifier depending on the value of R_{LDR}.

To compute the value of R_{LDR}, the second op-amp stage is analyzed. We can derive an expression for the current through the LED (or voltage across the LED V_{LED}) which is only dependent on the output voltage of the non-inverting amplifier. This equation then gives us the value of R_{LDR} for a specific LED current I_{LED} or voltage V_{LED}. The gain-equation for an inverting amplifier[5] is

$$g_{inv} = -\frac{R_B}{R_A} \quad . \tag{5}$$

If we apply this to the inverting amplifier around Q_2 (see Fig. 6), we know that the voltage at the output of Q_2 is

$$V_{inv} = -\frac{R_B}{R_A} \cdot V_{out} = -\frac{47\text{k}\Omega}{10\text{k}\Omega} \cdot V_{out} = -4.7 \cdot V_{out} \quad . \tag{6}$$

With this knowledge and the assumption that capacitor C_3 can be omitted for the static case, we can simplify the circuit to the series connection of R_7, two diodes D and the LED, as depicted in Fig. 6. This gives us an expression for the output voltage of the first op-amp stage with the non-inverting amplifier,

$$V_{\text{out}} = \frac{R_7 \cdot I_{\text{LED}} + 2 \cdot V_{\text{D}} + V_{\text{LED}}}{1 + 4.7} \quad . \tag{7}$$

As described in section 2.3, the current voltage characteristic of the diodes and the LED of the AOI have been measured and can now be used to solve Eq. 7 for every possible LED current. Eq. 4 can then be solved with the measured current resistance characteristic of the AOI and the input voltage to the corresponding output voltage can be calculated by solving

$$V_{\text{in}} = \frac{V_{\text{out}}}{g} \quad . \tag{8}$$

This leads to the static characteristic of the circuit, mapping the level of the input signal to the level of the output signal. This behavior is shown in Fig. 7. The solid line shows the result of the theoretic calculations which were derived from the circuit and the measurement of the electronic components. The dashed straight line indicates unity gain (output has the same level as input).

To see if the calculations were correct the static mapping curve of the circuit was also measured. A sine wave with a frequency of $f_0 = 1\,\text{kHz}$ with RMS levels from $-60\,\text{dB}$ to $6\,\text{dB}$ was sent through the circuit and the RMS level of the output signal was measured. The resulting curve is shown in Fig. 7. It matches the theoretical static curve very closely except for input signal levels between $-15\,\text{dB}$ and $-5\,\text{dB}$, where the measured curve deviates slightly from the calculated one. This deviation originates from the assumption of ideal operational amplifiers during the calculation of the static curve. When measuring the static curve with a higher supply voltage ($V_{cc} \approx 20\,\text{V}$), the error between calculated and measured curves decreases because the operational amplifiers are clipping at higher signal levels.

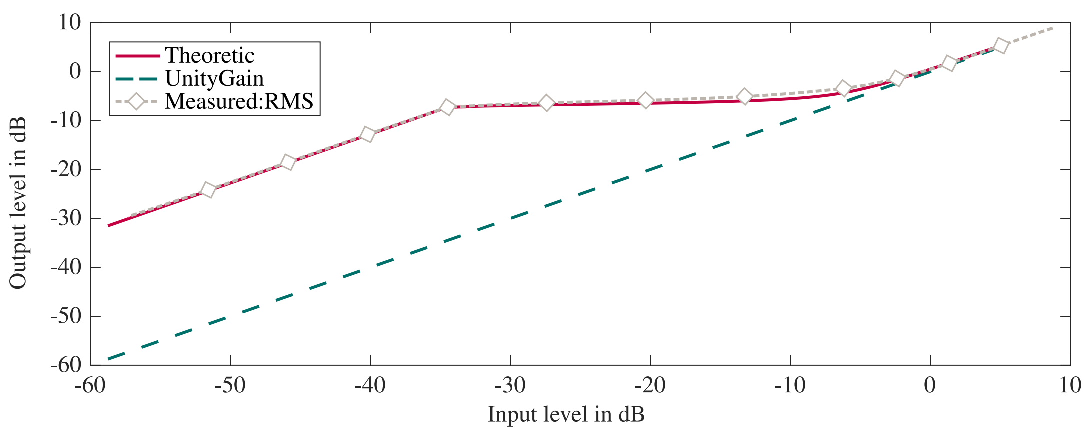

Figure 7: Static Mapping Curve: Calculated and Measured.

2.4.2 Dynamic Behavior

The dynamic behavior of a compression system describes how the system reacts to sudden changes of the input signal. It is divided into two parts. First, the attack behavior describes how the compression system reacts to a sudden rise in the level of the input signal. Second, the release behavior describes how the system reacts to a sudden drop (decrease) of the input signal level. When the signal level drops, the current through the LED decreases and the light intensity inside the opaque enclosure of the optocoupler reduces. The value of the resistance at the second port of the VTL5C2 is now increasing nonlinearly over time, depending on the physical properties of the optocoupler, thus increasing the resistance of the LDR and hence the gain value of the non-inverting operational amplifier stage. To illustrate this behavior, measurements for the 'turn-on' and 'turn-off'

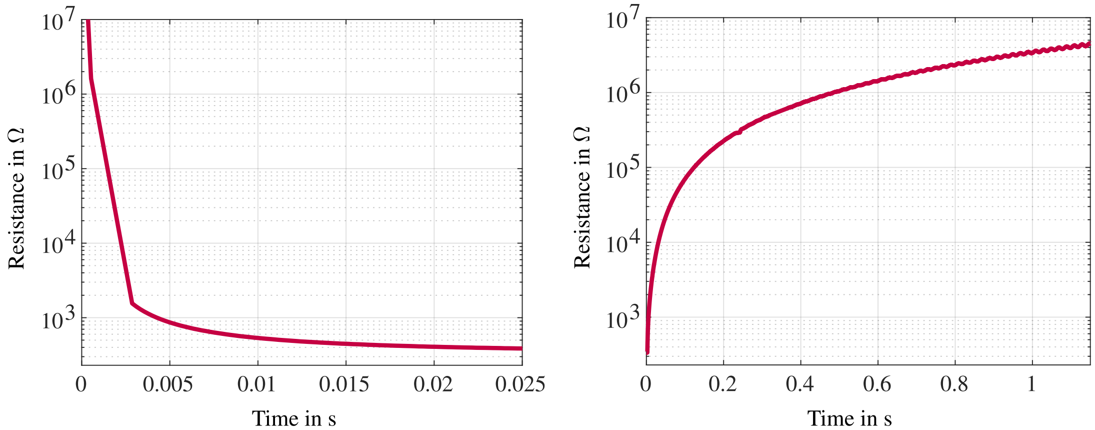

(a) (b)

Figure 8: Measurements of the VTL5C2 (a) turn-on resistance over time and (b) turn-off resistance over time.

case were done. First the current through the LED was switched from $i_{\mathrm{LED}} = 0\,\mathrm{mA}$ to $i_{\mathrm{LED}} = 10\,\mathrm{mA}$ at $t = 0\,\mathrm{s}$, as shown by Fig. 8a, and the resistance of the LDR was measured over time. The resistance of the LDR drops relatively fast. After $t = 5\,\mathrm{ms}$ the resistance of the LDR has already decreased below $R_{\mathrm{LDR}} < 1\,\mathrm{k\Omega}$. The change in resistance is so big in the first milliseconds that the measurement equipment (Keithley 2602B Source Meter) is not fast enough to track the value of the resistance between $t = 2\,\mathrm{ms}$ and $t = 3\,\mathrm{ms}$.

The measurement was repeated for the turn-off case. The current through the LED was switched from $i_{\mathrm{LED}} = 10\,\mathrm{mA}$ to $i_{\mathrm{LED}} = 0\,\mathrm{mA}$ at $t = 0\,\mathrm{s}$ and the resistance was measured over time as shown by Fig. 8b. In this case the LDR reacts much slower to the change of i_{LED}. After $t = 500\,\mathrm{ms}$ the resistance has risen to a value of $R_{\mathrm{LDR}} > 1\,\mathrm{M\Omega}$, which is 100 times longer than the turn-of case. To compare the behavior of the AOI with the

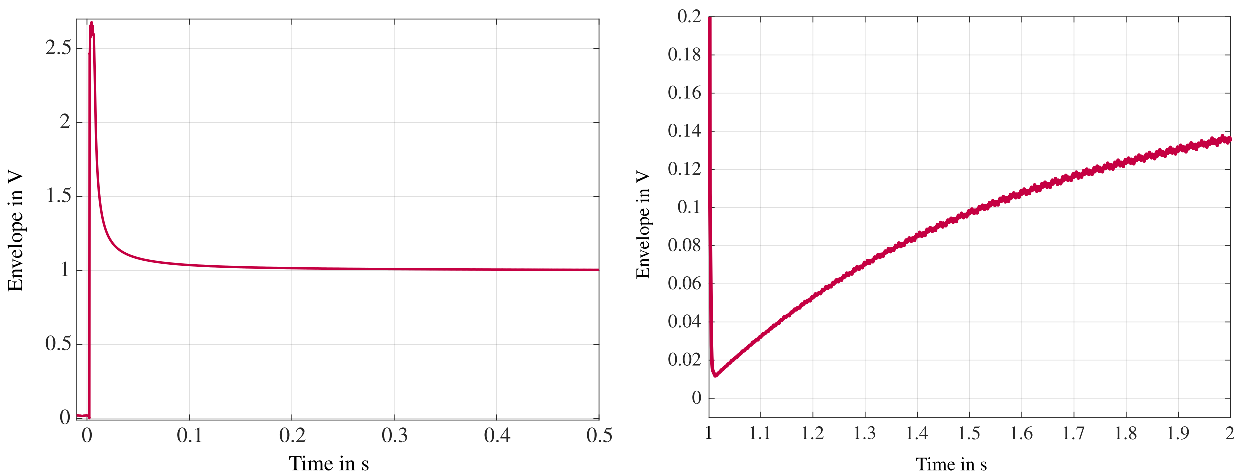

(a) (b)

Figure 9: Measurements of the reference device (a) attack and (b) release behavior over time.

behavior of the whole circuit, a sine wave with fundamental frequency $f_0 = 1000\,\mathrm{Hz}$ and an alternating amplitude was sent through the reference device. The amplitude of the input signal suddenly increases to $a = 1\,\mathrm{V}$ at $t = 0\,\mathrm{s}$ and drops down to $-40\,\mathrm{dBV}$ or $0.01\,\mathrm{V}$ after $t = 1\,\mathrm{s}$.

Figure 9a shows the envelope of the output signal for the attack case. But in comparison to Fig. 8a, the whole circuit reacts slower. The steady-state is reached after $t > 100\,\text{ms}$, which is 10 times longer than the reaction time of the AOI. This behavior directly corresponds to the value of the capacitor C_3, which is parallel to the LED of the AOI. This capacitor is smoothing the voltage across the LED, but also varies the attack-time of the reference device. The attack-time is proportional to the capacitance of C_3. Larger values yield a longer attack time, because it takes the capacitor more time to charge.

In the release phase, after a sudden drop of the input level, the AOI is the dominating element. When comparing Fig. 8b and Fig. 9b, the envelope of the reference output corresponds to the measurement of the LDR resistance.

The measured curves for attack and release behavior of the circuit are dependent on the characteristics of C_3 and the VTL5C2. A change in these characteristics, e.g. due to production tolerances, would lead to a different attack and release behavior. To be able to capture the behavior for reference devices with different characteristics, we chose to iteratively optimize the parameters of a digital model.

3. MODEL

The model we chose to emulate the reference system is a generic compressor model which can be seen in Fig. 10. It consists of a main path and a side-chain, which is used to calculate the variable gain $g(n)$ with which input

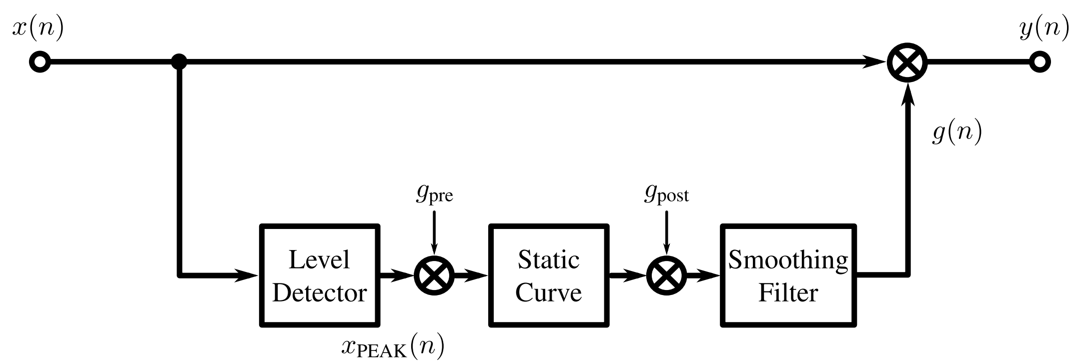

Figure 10: Generic compressor model.

signal $x(n)$ is multiplied. The first side-chain block is used to measure the level of the input signal and can be configured to give either the peak-level $x_{\text{PEAK}}(n)$ or the root mean square (RMS) level of the input signal $x_{\text{RMS}}(n)$.[6] Since the control voltage for the LED of the AOI is created by full-wave rectification and additional smoothing (low-pass filtering) of the audio signal, we employed the peak level-detector. The absolute value of the input signal is calculated and smoothed by a first order digital low-pass filter,

$$x_{\text{PEAK}}(n) = [(1-c) \cdot |x(n-1)| + c \cdot |x(n)|] \quad . \tag{9}$$

The value of the coefficient c depends on the level of the input signal. If $|x(n-1)| < |x(n)|$, the attack coefficient is chosen and the release coefficient in the opposite case $|x(n-1)| > |x(n)|$.[7] Additionally the level detector has different attack and release coefficients depending on the sign of the previous sample. If the sign of the previous sample is negative, different attack and release coefficients are chosen than for a positive sign of the previous sample. This enables us to emulate odd harmonics in the spectrum of the output signal.

The second block contains a lookup-table with a mapping curve for the steady state. The level of the input signal is mapped to the gain factor. In this work, the mapping curve was measured by sending multiple sine waves with $f_0 = 1000\,\text{Hz}$, $t = 0.5\,\text{s}$ length and signal levels from $-80\,\text{dB}$ to $6\,\text{dB}$ through the reference device

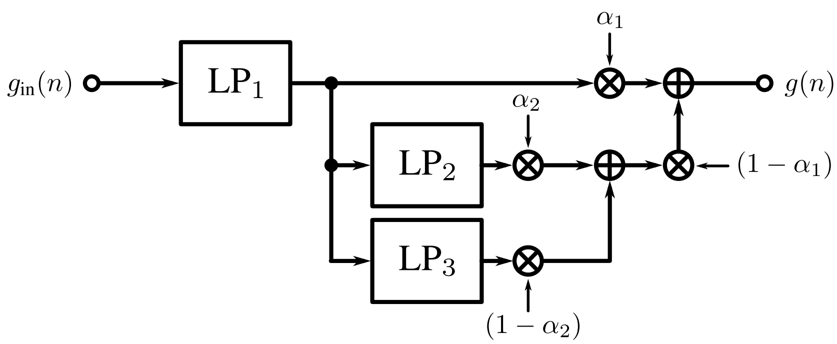

Figure 11: Block diagram of the smoothing filter.

and measuring the level of the output signal. Afterwards the gain-curve can be calculated with the help of Eq. 8. The gain parameters g_{pre} and g_{post} can be used to scale the gain curve for enhanced flexibility of the model.

The third block is a combination of low-pass filters with different coefficients for attack and release case. It is used for smoothing of the gain factor because humans perceive it as unpleasant if the gain value $g(n)$ alters too quickly over time. The filter is a combination of three first order low-pass filters, which allows more flexibility, when the model is adapted to the measurements of the reference device. Figure 11 shows how the filters are combined. The weights $\alpha_1 \in [0, 1]$ and $\alpha_2 \in [0, 1]$ ensure that no energy is lost or added, when combining the filters.

3.1 Extended Model

The generic model from the previous section does not attenuate any frequency components of the input signal. But the circuit of the compressor contains input and output filters (capacitors C_1 and C_2 with their corresponding resistances). For this reason we extended the generic model with a linear time invariant filter, to properly model

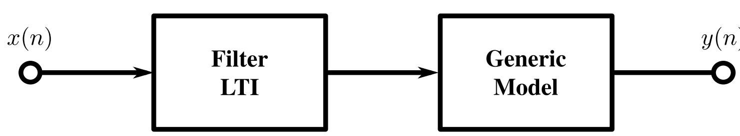

Figure 12: Extended compressor model.

the frequency dependency of the system. Fig. 12 illustrates the performed extension. The measurement of the impulse response is described in the next section.

4. FILTER IDENTIFICATION

As described by Farina, the linear part of the circuit is measured with an exponentially swept sine.[8] All measurements were done with a common sampling rate for audio data of $f_s = 48\,\text{kHz}$. The system is excited within a certain frequency range by sending the exponentially swept sine wave through the reference system. The sweep

$$x_{\text{sweep}}(n) = A \cdot \sin\left(\omega_1 \cdot \frac{N}{\ln\left(\frac{\omega_2}{\omega_1}\right)} \cdot \left[\mathrm{e}^{\frac{n}{N}\cdot\ln\left(\frac{\omega_2}{\omega_1}\right)} - 1\right]\right), \tag{10}$$

has a duration of N samples, a maximum amplitude of A and covers frequencies from $\omega_1 = 2\pi f_{\text{start}}/f_s$ to $\omega_2 = 2\pi f_{\text{stop}}/f_s$. The amplitude was set to $A = 0.01\,\text{V}$ to ensure that no dynamic range compression of the input signal occurs. To extract the impulse response an inverse filter x_{inv} is designed which yields a Dirac-delta function (that is only scaled and shifted in time) when it is convolved with the original sweep,

$$x_{\text{sweep}}(n) * x_{\text{inv}}(n) \approx c \cdot \delta(n - n_0) \tag{11}$$

with

$$x_{\text{inv}}(n) = x_{\text{sweep}}(N - 1 - n) \cdot (\omega_2/\omega_1)^{\frac{-n}{N-1}}. \tag{12}$$

Where N is the total amount of samples and ω_1 and ω_2 are the start and stop frequencies. Convolving the output of the reference circuit $y_{\text{sweep}}(n)$ with the inverse filter $x_{\text{inv}}(n)$ yields the small signal impulse response $h(n)$ of the circuit

$$h(n) = \frac{1}{c} \cdot x_{\text{inv}}(n) * y_{\text{sweep}}(n). \tag{13}$$

The time shift from Eq. 11 has to be compensated and the filter is normalized in frequency domain to have a maximum Magnitude of 0 dB. This is done, because the filters in the circuit are first order passive low-pass resp. high-pass filters, which do not amplify the signal. The result of the filter measurement is directly used as a finite impulse response (FIR) filter in the extended model. The measured frequency response can be seen in Fig. 13. The influence of the RC high-pass filters at the input and output of the circuit can be seen for frequencies below

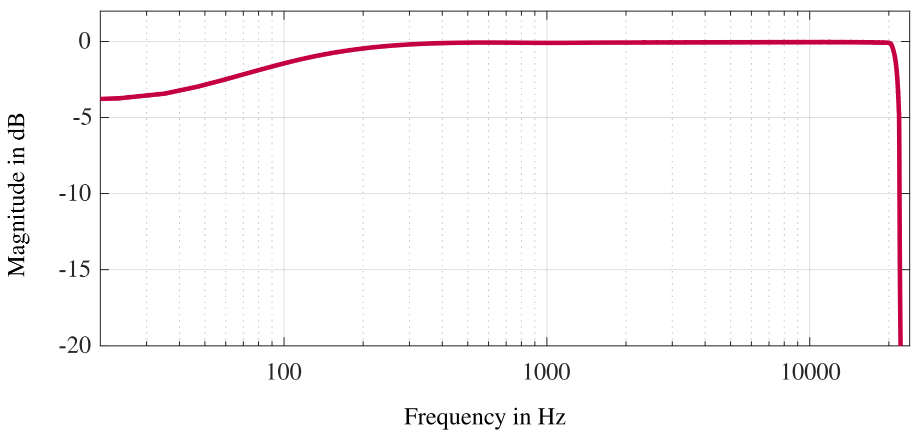

Figure 13: Linear frequency response of the reference system.

100 Hz. The frequency response for high frequencies is flat up to 20 kHz. Above 20 kHz the frequency response is band-limited to avoid unwanted aliasing effects due to frequency components of the input signal which might be above the Nyquist frequency $\frac{f_s}{2}$.

5. ITERATIVE OPTIMIZATION

To be able to adapt the digital model in any case, e.g. with different circuit components of the dynamic range compressor, or even other dynamic range compression devices, iterative optimization of the model parameters has been performed. As Fig. 14 illustrates, specific test signals are sent through reference system and digital model. The output of the system $y_{\text{sys}}(n)$ and the output of the model $\hat{y}_{\text{mod}}(n, \mathbf{p})$ are given to a parameter estimation algorithm which calls a cost function, calculating the residual between reference and simulation. The output of the model does not only depend on the value of the input signal $x(n)$, but also on the parameter vector $\mathbf{p}$. Depending on the employed parameter estimation algorithm and the result of the cost function, the

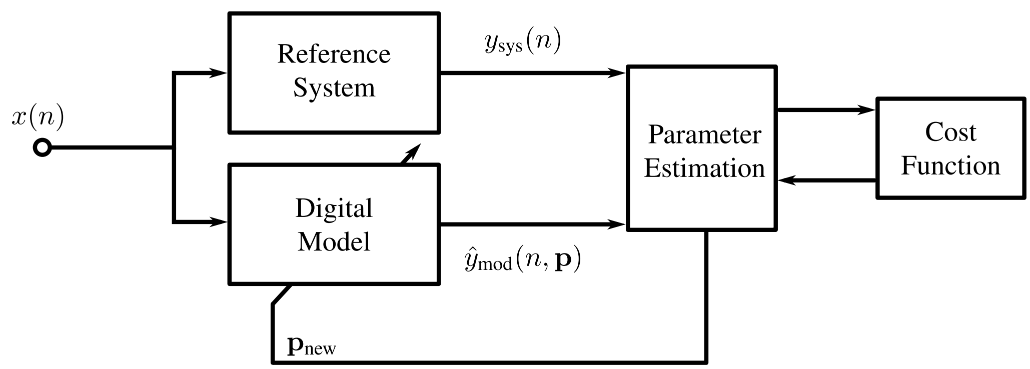

Figure 14: Optimization scheme with cost function.

parameter vector is updated to $\mathbf{p}_{\text{new}}$, the model output is recalculated and the cost function is evaluated again. Please note that the digital to analog conversion (DAC) and the analog to digital conversion (ADC) before and after the analog reference system are omitted due to readability.

The parameter estimation algorithm which was used in this work is the Levenberg–Marquardt algorithm.[9,10] It is a gradient-based technique, which gives very good results if the cost function does not have local minima and if the initial parameter set is not too far from the global solution. Since the algorithm is gradient-based it is possible to get stuck in a local minimum during optimization. The signals and techniques used in this work to have a robust identification of the parameters are presented in the following.

5.1 Steady State: Gain Matching

The static curve in the side-chain of the digital model (see Fig. 10) maps the level of the input signal $x(n)$ to a specific gain value $g(n)$. It has been measured and stored in a lookup-table. But to allow more flexibility during

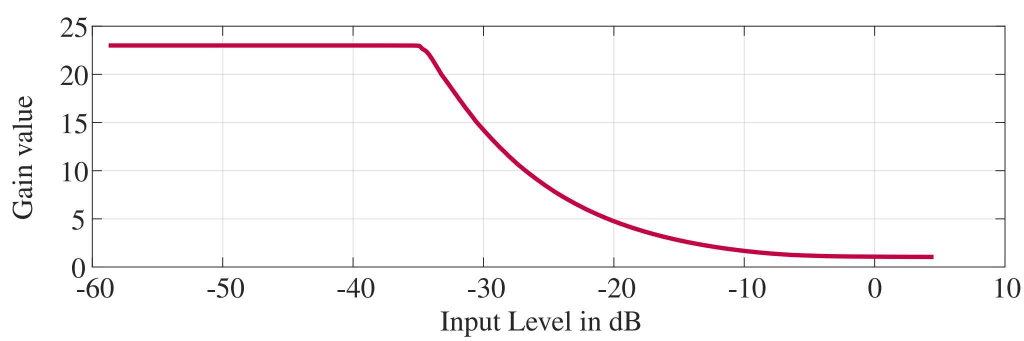

Figure 15: Mapping curve – Input level to gain value.

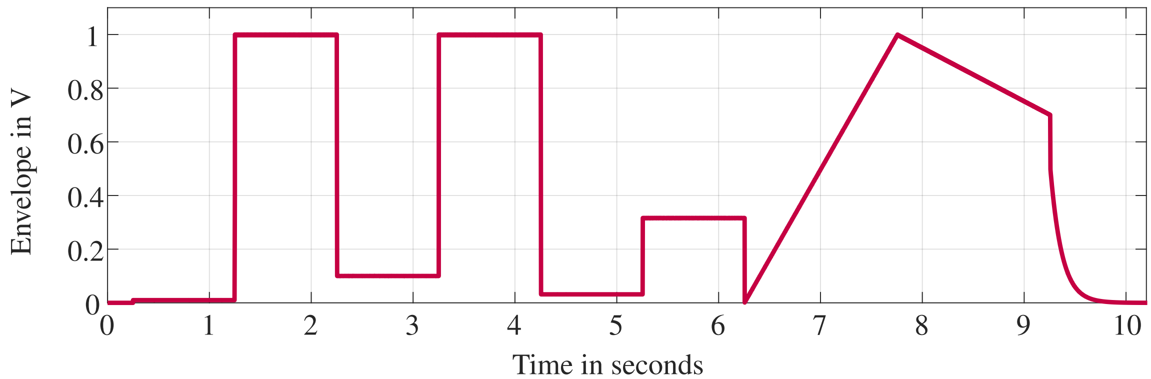

Figure 16: Time-domain plot of $a(n)$.

optimization the gains g_{pre} and g_{post} have been added directly before resp. after the static curve. With variation of the pre-gain g_{pre}, the static curve (see Fig. 15) can be shifted along the input-level axis and variation of the post-gain g_{post} allows scaling of the curve for the gain value axis.

In the first optimization step an amplitude modulated sine wave is sent through the reference device and the output is recorded. The sine signal can be modified to feature varying envelopes

$$x_{\mathrm{sin,var}}(n) = a(n) \cdot \sin\left(2\pi \frac{f_0}{f_s} n\right), \tag{14}$$

where $a(n)$ is a time-variant amplitude. As shown by Fig. 16, $a(n)$ varies abruptly between several amplitude values as well as gradual linear variation of amplitude. The signal ends with an exponentially decaying envelope, as it is common for plucked string instruments. The only parameters which can be altered during this first optimization step are g_{pre} and g_{post}. They are initialized to have a value of $g_{\mathrm{pre}} = g_{\mathrm{post}} = 1$.

The cost function for this optimization step is the difference of the envelopes of reference output and model output. First, the envelopes of reference output and model output are calculated with a peak-picking technique, then the difference between their logarithmic values is calculated. The sum of absolute values of this residual yields the result of the cost function which has to be minimized.

The employed peak-picking technique works in several steps. At first, the signal is divided into positive and negative amplitudes by copying the signal and setting all negative (resp. positive) values to zero. Afterwards the peaks of the original signal are found by locating the sign changes of the first derivative. The value of the signal at this location is extracted and finally all the extrema are connected by linear interpolation.

5.2 Matching of Dynamic Parameters

The dynamic parameters are the coefficients of the first order low-pass filters in the level detector and smoothing filter of the digital model. The adaption of these parameters is carried out in two steps. First, the amplitude modulated sine wave from section 5.1 is used as an input signal and all dynamic parameters are adapted at once. Second, an application specific input signal is chosen and the dynamic parameters are refined separately for attack and release case. The cost function computes the difference of the envelopes of both output signals, as for the previous gain optimization step.

The adapted model should be used with signals from electric guitars, electric basses or recordings of them. Therefore an appropriate input signal was designed, which is shown in Fig. 17. A decaying tone played by an electric bass guitar starts the signal as far as 3.1 seconds, followed by single notes and a decaying chord, played by an electric guitar up to 6.9 seconds. The last second of the signal consists of a short drum recording with bass-drum, snare-drum and hi-hat sounds. Especially the drum part of the input signal helps identifying the dynamic parameters of the model due to the transient characteristic of the instrument.

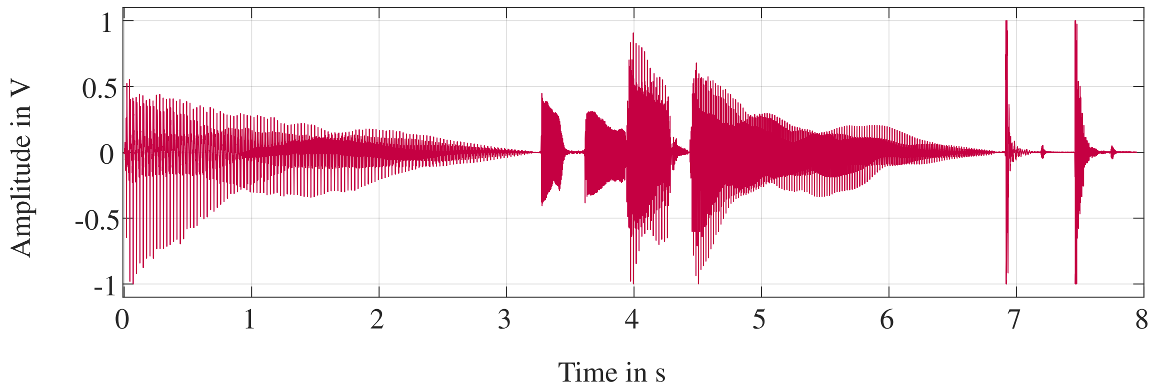

Figure 17: Time-domain plot of the input signal.

In the first optimization of the dynamic parameters, the amplitude modulated sine input helps getting a good initial estimate for the dynamic parameters, but if the model would only be adapted to this relatively simple input signal, attack and release behavior would not yield satisfactory results if an input signal from an electric guitar would be processed. Therefore the second optimization step for the dynamic parameters is needed to adapt attack and release coefficients of the digital model to a real-world signal.

The final optimization step is needed to refine the parameters of the digital model. The cost function is now calculating the unnormalized mean square error in time-domain (shown by the numerator of Eq. 15). Because the parameters are already close to the optimal solution, this optimization step can further improve the modeling result. After this last step the digital model is successfully adapted to the reference system.

6. DISCUSSION

It is very difficult to rate the quality of the model with objective scores, because they do not necessarily represent the perceptual quality for a human listener. If the difference of the recorded reference output and adapted digital model output is simply calculated in time-domain, a small phase shift between both signals would yield a non-negligible error. But perceptually the model could be indistinguishable from the reference device.

6.1 Metrics Definition

For this reason we chose several metrics for the assessment of the quality of the adapted model. The first metric would be the 'error to signal ratio' or ESR. It represents the amount of the error energy in relation to the energy of the reference signal. But the error is still calculated in time-domain,

$$\mathrm{ESR} = \frac{E_{\mathrm{res}}}{E_{\mathrm{sys}}} = \frac{\sum\limits_{n=-\infty}^{\infty} \left|y_{\mathrm{sys}}(n) - \hat{y}_{\mathrm{mod}}(n, \mathbf{p})\right|^2}{\sum\limits_{n=-\infty}^{\infty} \left|y_{\mathrm{sys}}(n)\right|^2}. \tag{15}$$

If the value described by Eq. 15 is close to zero, the energy of the error is very small in relation to the energy of the signal. If the value is close to one, the model is definitely not well adapted, since the energy of the error signal is close to the signal energy.

The second metric we used to describe how close the adapted model can represent the reference system is the correlation coefficient. It describes the linear dependence of two random variables. The correlation coefficient $\rho(\mathrm{X,Y})$ is computed by

$$\rho(\mathrm{X,Y}) = \frac{\mathrm{cov(X,Y)}}{\sigma_{\mathrm{X}}\sigma_{\mathrm{Y}}}, \tag{16}$$

Impairment description	ODG
Imperceptible	0
Perceptible, but not annoying	-1
Slightly annoying	-2
Annoying	-3
Very annoying	-4

Table 1: Impairment description and corresponding objective difference grade (ODG) according to ITU-R BS.1387-1.[11]

where cov(X,Y) is the covariance of X and Y, $y_{\mathrm{sys}}(n) = X$ and $\hat{y}_{\mathrm{mod}}(n, \mathbf{p}) = Y$ are random variables which represent the output signals of reference system and digital model respectively and σ represents the standard deviation of the random variables.

The third metric is the objective difference grade (ODG), which originated from recommendation BS.1387-1 by the international telecommunication union (ITU), an algorithm for objective measurements of perceived audio quality, also called PEAQ.[11] It was developed to objectively evaluate the quality of audio codecs to reduce the need for a time-consuming listening test with human participants. Table 1 shows the impairment description and the corresponding ODG score. If the ODG is between 0 and -1 the differences in the signals are not perceptible for a human listener. If the score is close to -1 or even lower, the difference between the two signals are barely audible and can only be detected by a trained listener. As Wey et al. have shown, an mp3 file with a bitrate of $b = 128\,\mathrm{kbps}$ has an ODG score of about $ODG \approx -1$ and with $b = 256\,\mathrm{kbps}$ $ODG \approx -0.3$ for comparison.[12] To compute the ODG score between the analog reference system and the adapted digital model, the 'GstPEAQ' implementation of Holters was used in its 'basic' variant.[13]

6.2 Results

To see how well the model was adapted to the reference device, the scores described in section 6.1 were calculated for different input signals. The first two input signals were the signals used during optimization. The variable amplitude sine wave and the application specific test signal (described in sections 5.1 and 5.2). Afterwards independent signals, which were not used during optimization, are tested to see if the model gives good results for different inputs. The independent signals are recordings from an electric guitar resp. bass, without any processing. The instruments were connected to an audio interface and their output was directly recorded. The amplitude of the recordings has been normalized to 0 dB, because the whole amplitude range from $-1\,\mathrm{V}$ to $1\,\mathrm{V}$ should be covered by the input signals to see if the model behaves appropriately for every possible input amplitude.

#	Signal	ESR	ρ(X,Y)	ODG
1	$x_{\mathrm{sin,var}}(n)$	0.0091	0.9955	-1.596
2	Optimization signal (Guitar,Bass,Drums)	0.0187	0.9907	-0.458
3	Guitar	0.0174	0.9913	-0.456
4	Bass (Low pitch)	0.024	0.988	-0.332
5	Bass (High pitch)	0.0326	0.9837	-0.742

Table 2: Quality of the adapted digital model. Objective scores.

The first signal $x_{\mathrm{sin,var}}(n)$ has a very good error to signal ratio of ESR $< 1\%$ and a high correlation coefficient of $\rho = 0.9955$, but the ODG score for this synthetic signal has a low value of ODG $= -1.596$. The optimization signal consisting of electric guitar, electric bass guitar and drums has an ESR $< 2\%$ and a lower correlation coefficient of $\rho = 0.9907$, but ODG $= -0.458$. This indicates that the ESR and $\rho(X, Y)$ are not very well suited to describe the perceptual error between two signals. On the other hand, the ODG score is not well suited as a cost function because it behaves very nonlinear, which is not desirable when using gradient-based optimization schemes like Levenberg–Marquardt. Another reason for the better ODG score of input 2 could be the optimization routine. Because input 2 is the last input signal the parameters of the digital model are optimized for, it has a better ODG score than input 1.

The independent test inputs 3–5 all have similar ESR and $\rho(X, Y)$ values. The ODG score is slightly worse for the bass guitar with a high position on the fingerboard. But due to the psycho-acoustical processing of the PEAQ algorithm, errors for low-pitched sounds might not be weighted as much as for higher pitched-sounds.

In general, the results of the optimization process are very good. No ODG score below -1 could be detected for electric guitar or bass guitar inputs. This means that the output of the digital model is still different from the output of the reference system but the difference is barely noticeable.

To visually illustrate how well the digital model fits the reference device, a time-domain plot from the drum part of the optimization signal is shown by Fig. 18. This part of the signal is very transient, so any false

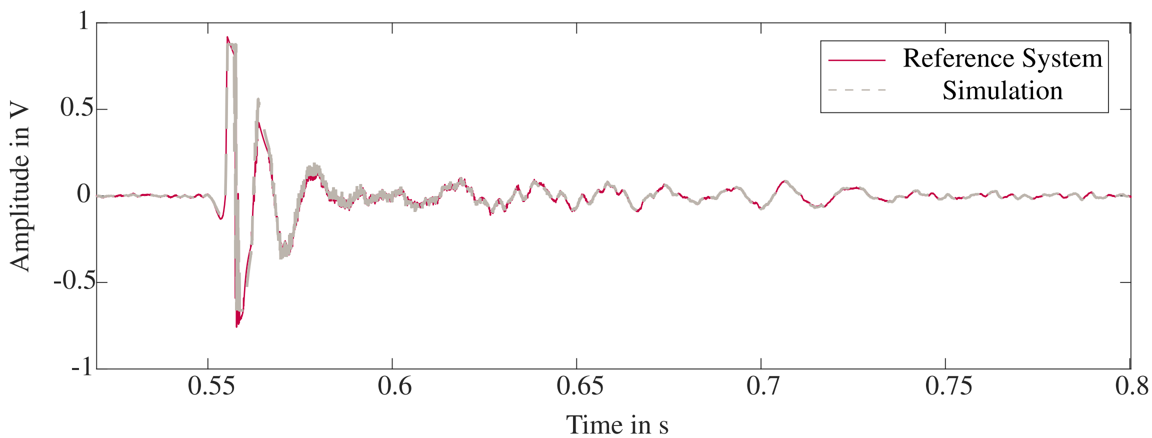

Figure 18: Time-domain comparison of reference and simulation for bass drum input.

optimization of the dynamic parameters would be visible. The digital model, as shown by the dashed line in Fig. 18, follows the reference system very well.

7. CONCLUSION

In this work, a generic digital dynamic range compressor model has been successfully adapted to an analog reference device which is using the properties of an analog optical isolator to achieve dynamic range compression. The model is adapted to the reference device in several steps. First the linear response of the circuit is measured and modeled, then the steady state behavior of the circuit is measured and used in the digital model. Finally the parameters of the digital model are optimized in several steps and for different input signals.

The benefit of adapting the model with system identification techniques is the flexibility of this method. With proper input/output measurements, every dynamic range compression device can be emulated. Although it has been done in this work, the proposed approach does not need extensive circuit analysis or even time-consuming reverse-engineering of an unknown circuit.

The results still show room for improvement although only an experienced listener will be able to hear the difference between digital simulation and analog reference. To optimize the results for a human listener, a psycho-acoustic motivated cost function could yield better results. But the result of the cost function has to be proportional to the perceived error value. For the PEAQ algorithm the ODG value behaves not proportional because it saturates for very bad and very good results which makes iterative optimization nearly impossible.

REFERENCES

[1] UREI, *Model LA-2A Leveling Amplifier: User's Guide* (1979).

[2] Hollis, J., "Assorted circuit designs." http://www.hollis.co.uk/john/circuits.html (2001). [Online; accessed 5-January-2016].

[3] Kröning, O., Dempwolf, K., and Zölzer, U., "Analysis and simulation of an analog guitar compressor," in [*Proc. of the 14th Int. Conference on Digital Audio Effects (DAFx-11)*], 205–208 (Sep 2011).

[4] Perkin Elmer, *Photoconductive Cells and Analog Optoisolators* (2001).

[5] Kories, R. and Schmidt-Walter, H., [*Taschenbuch der Elektrotechnik*], vol. 8, Wissenschaftlicher Verlag Harri Deutsch GmbH (2008).

[6] Zölzer, U., [*DAFX: Digital Audio Effects*], vol. 2, Wiley Online Library (2011).

[7] Giannoulis, D., Massberg, M., and Reiss, J. D., "Digital dynamic range compressor design – a tutorial and analysis," *Journal of the Audio Engineering Society* **60**(6), 399–408 (2012).

[8] Farina, A., "Simultaneous measurement of impulse response and distortion with a swept-sine technique," in [*Audio Engineering Society Convention 108*], (February 2000).

[9] Levenberg, K., "A method for the solution of certain problems in least squares," *Quarterly of applied mathematics* **2**, 164–168 (1944).

[10] Marquardt, D. W., "An algorithm for least-squares estimation of nonlinear parameters," *Journal of the Society for Industrial & Applied Mathematics* **11**(2), 431–441 (1963).

[11] International Telecommunication Union, "Bs.1387: Method for objective measurements of perceived audio quality." Available online at http://www.itu.int/rec/R-REC-BS.1387 – accessed July 18th 2016.

[12] Wey, H.-S., Ito, A., Okamoto, T., and Suzuki, Y., "Multiple description coding for an mp3 coded sound signal," in [*Proc. of 20th International Congress on Acoustics, ICA*], (2010).

[13] Holters, M. and Zölzer, U., "Gstpeaq – an open source implementation of the peaq algorithm," in [*Proc. of the 18th Int. Conference on Digital Audio Effects (DAFx-15)*], (Dec. 2015).